

Influence of Low-Symmetry Distortions on the Luminescence of Cr^{4+} -Doped Forsterite

Yongrong Shen and Kevin L. Bray

Department of Chemistry, Washington State University, Pullman, Washington 99164-4630

(Received 22 November 1999)

By using pressure to vary the extent of nontetrahedral distortions of the Cr^{4+} site in Mg_2SiO_4 , we reveal the important influence of the 3T_1 state on the emission properties of the 3T_2 state. We find that 3T_1 - 3T_2 mixing has a pronounced effect on the line shape and radiative decay rate of emission from the 3T_2 state and that the extent of mixing depends critically on the magnitude of nontetrahedral distortions. The results provide an explanation for the wide variation of Cr^{4+} emission properties in different host lattices at ambient pressure and indicate that the tailoring of asymmetric distortions of luminescent centers represents an effective new strategy for tuning the linewidth of spectral transitions.

PACS numbers: 78.55.Hx, 62.50.+p, 71.70.Ch

Recent work on near-infrared (NIR) tunable solid state laser materials has focused on the dopant Cr^{4+} in several host lattices with $\text{Cr}^{4+}:\text{Mg}_2\text{SiO}_4$ emerging as the leading technological system. The success of $\text{Cr}^{4+}:\text{Mg}_2\text{SiO}_4$ as a tunable NIR laser material [1] has stimulated numerous recent studies of the spectroscopic properties of Cr^{4+} [2–9] and other $3d^2$ dopants (Mn^{5+} , Fe^{6+}) [10–14] because of the need for new NIR optical materials. Current work on $\text{Cr}^{4+}:\text{Mg}_2\text{SiO}_4$ continues to focus on tunable NIR laser applications [15], as well as applications in frequency doubled visible [16] and ultrafast lasing [17].

The desirable optical properties of Cr^{4+} are accompanied by puzzling questions on the origin of the luminescence. To date, the electronic structure of Cr^{4+} has proven to be elusive because of confusion over the energy and spectroscopic properties of the 1E and 3T_2 excited states. The two states are predicted to be close in energy and have both been implicated in the NIR emission properties of Cr^{4+} . Difficulties in understanding the behavior of Cr^{4+} in Mg_2SiO_4 and other host lattices have led to considerable and oftentimes conflicting discussion in the literature [2,3,17,18] and suggest that previously unrecognized phenomena are contributing to the optical properties of Cr^{4+} . As a result, the experimental determination of the electronic structure of Cr^{4+} , its influence on optical properties, and its relationship to local structure present new opportunities for extending our ability to design and control the properties of optical materials.

In this Letter, we demonstrate the role of nontetrahedral local structural distortions in determining the electronic structure and luminescence properties of Cr^{4+} in Mg_2SiO_4 . By using high pressure to systematically increase the deviation of Cr^{4+} from regular tetrahedral symmetry, we show that nontetrahedral distortions induce 3T_2 - 3T_1 excited state coupling and that the strength of this coupling controls the ambient pressure ${}^3T_2 \rightarrow {}^3A_2$ emission line shape and radiative decay rate. We also establish the energy of the 1E excited state and show that it does not contribute to the ambient pressure luminescence.

Cr^{4+} substitutes for Si^{4+} in Mg_2SiO_4 and occupies a distorted tetrahedral site with formal C_s and approximate C_{2v} site symmetry [2,3,18–20]. High pressure NIR luminescence experiments [21] on $\text{Cr}^{4+}:\text{Mg}_2\text{SiO}_4$ were performed as a function of pressure up to 225 kbar at 40 K. All spectra in this paper were corrected for instrumental response and normalized to their peak intensity. Figure 1 shows representative luminescence spectra below ~ 70 kbar at 40 K. The ambient pressure spectrum consisted of an intense sharp line around 1094 nm with weak vibronic sidebands and has been assigned to the transition from the lowest C_{2v} spin-triplet crystal field (CF) component [$({}^3T_2)({}^3B_1)$] of the 3T_2 excited state [22] to the 3A_2 ground state [$({}^3A_2)({}^3A_1)$] [2,19,20,22,23]. In the higher resolution scan at ambient pressure (Fig. 1b), the intense line around 1094 nm was observed to consist of three distinct features at 1089.4 nm (9179 cm^{-1}), 1091.5 nm (9162 cm^{-1}), and 1093.2 nm (9147 cm^{-1}). The three features are a consequence of a spin-orbit coupling induced fine splitting. Upon application of pressure, a strong blueshift of the luminescence lines was observed. The blueshift was similar

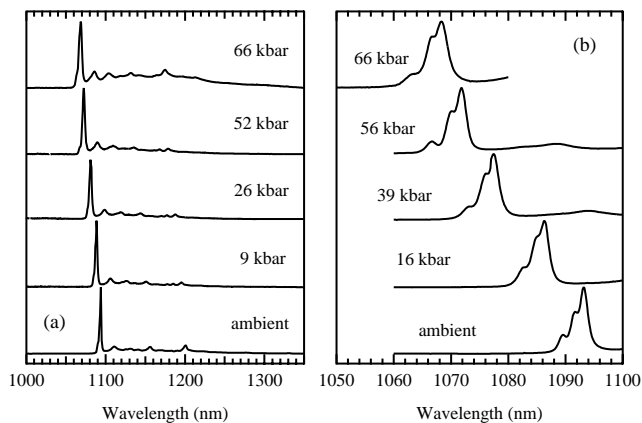


FIG. 1. Luminescence spectra ($\lambda_{\text{ex}} = \sim 620$ nm) of $\text{Cr}^{4+}:\text{Mg}_2\text{SiO}_4$ at 40 K between ambient pressure and 66 kbar.

for all three components and was linear up to ~ 70 kbar [$3.4(2) \text{ cm}^{-1}/\text{kbar}$]. We also observed a linear decrease in the 20 K lifetime from $30(1) \mu\text{s}$ at ambient pressure to $15(2) \mu\text{s}$ at 66 kbar.

Between ~ 70 and ~ 120 kbar, the magnitude of the blueshift progressively decreased (Fig. 2a). The change in shift behavior was accompanied by a gradual spectral transformation from the narrow luminescence observed at low pressure to a broad, longer wavelength luminescence band. We analyzed the change in spectral line shape using a single configurational coordinate (SCC) model [24] (Fig. 3). The corresponding values of the Huang-Rhys factor (S) and phonon energy ($\hbar\omega$) are $S = 1.84(4)$, $\hbar\omega = 419(8) \text{ cm}^{-1}$ at 92 kbar; $S = 1.87(5)$, $\hbar\omega = 430(9) \text{ cm}^{-1}$ at 99 kbar; and $S = 2.24(7)$, $\hbar\omega = 434(11) \text{ cm}^{-1}$ at 122 kbar for the pressure-induced broadband. For comparison purposes, values of S up to ~ 3 and coupling phonon energies ranging from 393 to 450 cm^{-1} have been reported for broadly emitting Cr^{4+} ions in several oxide lattices at ambient pressure [5]. In addition to the broad luminescence band, we also continued to observe the zero-phonon (3T_2) 3B_1 line and several vibronic replicas present at low pressure. These features decreased in intensity relative to the broad emission upon increasing pressure (Fig. 3).

Above ~ 120 kbar, the intensity of the broad emission band decreased and a transformation to a new sharp line spectrum occurred (Fig. 2b). The principal new feature (E_1) was clearly evident at ~ 140 kbar and gained intensity at higher pressure, as the broad luminescence intensity decreased. The E_1 line exhibited a small blueshift ($\sim 0.3 \text{ cm}^{-1}/\text{kbar}$) between ~ 140 and ~ 200 kbar and a small redshift (about $-0.69 \text{ cm}^{-1}/\text{kbar}$) above ~ 200 kbar.

Quantitative modeling of the energy levels requires consideration of the effect of pressure on the cubic (T_d) and nontetrahedral crystal fields of Cr^{4+} in Mg_2SiO_4 . We have completed a calculation of the pure electronic energies

of the three spin-triplet states in T_d symmetry [$(e_t)_2{}^3T_2$, $(e_t)_2{}^3T_1$, and $(t_2^2){}^3T_1$] in the framework of a nontetrahedral geometric distortion scheme $T_d \rightarrow D_{2d} \rightarrow C_{2v}$. Within this scheme, we introduced the tetragonal CF splitting parameters δ and μ to account for the reduction to D_{2d} symmetry and orthorhombic CF splitting parameters ν and ν' to account for the further reduction to C_{2v} symmetry. δ , μ , ν , and ν' are positive quantities in our calculation. We set up and solved the energy matrices corresponding to the distortion scheme to obtain the triplet state electronic energies as a function of nontetrahedral distortion.

In the approximate C_{2v} symmetry of $\text{Cr}^{4+}:\text{Mg}_2\text{SiO}_4$, each of the spin-triplet states splits into three CF levels (B_1 , B_2 , and A_2). In a first approximation which neglects $(e_t)_2$ - (t_2^2) configuration interaction, our calculation predicts that the states $|(e_t)_2{}^3T_2{}^3E{}^3B_1\rangle$ [25] and $|(e_t)_2{}^3T_1{}^3E{}^3B_1\rangle$ mix due to the nontetrahedral geometric distortion. The lowest energy triplet state in this approximation is calculated to be $|(e_t)_2{}^3T_2{}^3E{}^3B_1\rangle$ with the energy (E) and wave function (Ψ) given below:

$$E \approx 10Dq - \frac{1}{6}(2\delta + 3\nu) - \frac{1}{4}(\mu + 2\sqrt{3}\nu') - \frac{\chi^2}{|\kappa|}, \quad (1)$$

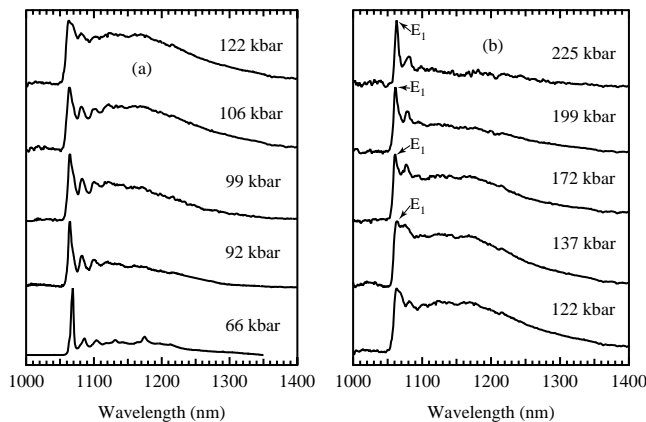


FIG. 2. Luminescence spectra ($\lambda_{\text{ex}} = \sim 620 \text{ nm}$) of $\text{Cr}^{4+}:\text{Mg}_2\text{SiO}_4$ at 40 K: (a) between 66 and 122 kbar and (b) above 122 kbar.

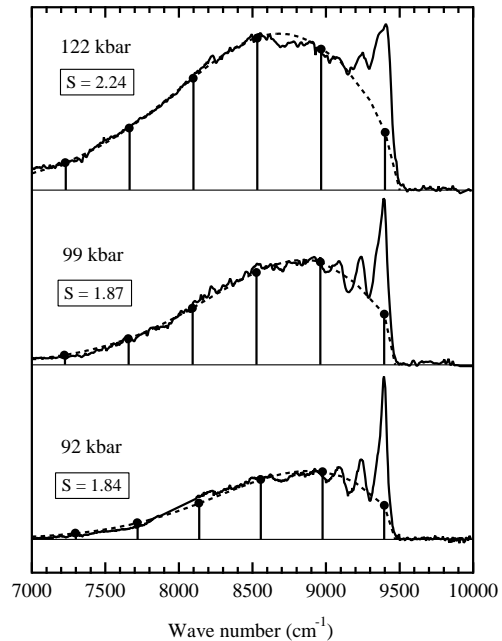


FIG. 3. Luminescence spectra of $\text{Cr}^{4+}:\text{Mg}_2\text{SiO}_4$ at 40 K and 92, 99, and 122 kbar. The vertical lines represent SCC intensity calculations of broad, low energy emission band stabilized by pressure. The dashed curves are a guide to the eye and provide an approximation of the line shape of the broad emission band. The sharp zero phonon (3T_2) 3B_1 and vibronic transitions observed at ambient pressure are also present between ~ 9000 and $\sim 9400 \text{ cm}^{-1}$ but decreased in intensity as the broad emission band was stabilized.

$$\Psi \approx \sqrt{1 - \left(\frac{\chi}{\kappa}\right)^2} |(et_2)^3T_2^3E^3B_1\rangle - \left|\frac{\chi}{\kappa}\right| |(et_2)^3T_1^3E^3B_1\rangle, \quad (2)$$

$$\chi = -\frac{1}{4}(\sqrt{3}\mu - 2\nu'), \quad \kappa = \frac{1}{2}(24B + \mu + 2\sqrt{3}\nu'),$$

where Dq is the cubic CF parameter and B is the Racah parameter.

Equation (1) indicates that the energy of the emitting $(^3T_2)^3B_1$ state at low pressure is influenced by both the cubic and nontetrahedral crystal fields. An increased cubic field leads to an increased $(^3T_2)^3B_1$ energy and an increased nontetrahedral field leads to a decreased $(^3T_2)^3B_1$ energy. Depending on the relative influence of pressure on the cubic and nontetrahedral crystal fields, a blueshift or a redshift of the emitting $(^3T_2)^3B_1$ state may occur. Since pressure increases the cubic CF strength, we expect a blueshift for the emitting state unless a compensating increase in the nontetrahedral distortion occurs.

Equations (1) and (2) provide insight into the luminescence behavior of $\text{Cr}^{4+}:\text{Mg}_2\text{SiO}_4$ with pressure. Below ~ 70 kbar, the observed blueshift ($-13.4 \text{ cm}^{-1}/\text{kbar}$) of the $(^3T_2)^3B_1$ state indicates that the cubic CF effect dominates the nontetrahedral distortion effect. Since, to our knowledge, the expected increase in $10Dq$ with pressure in a regular tetrahedral oxide system has not been reported, it is difficult to determine whether or not the observed blueshift is influenced secondarily by changes in the nontetrahedral distortion. The effect of pressure on cubic CF strength is best understood in studies of octahedral Cr^{3+} oxide systems which have shown that pressure has a negligible effect on noncubic distortions and consistently leads to increases in $10Dq$ of $\sim 10 \text{ cm}^{-1}/\text{kbar}$ [26–28]. Using $Dq(\text{tet}) = (4/9)Dq(\text{oct})$, we would expect a blueshift of $\sim 4.4 \text{ cm}^{-1}/\text{kbar}$ for the $(^3T_2)^3B_1$ state in the absence of pressure-induced changes in the nontetrahedral distortion. The smaller observed blueshift suggests that a small increase in distortion occurs with pressure below ~ 70 kbar. The observed decrease in lifetime below ~ 70 kbar is also consistent with an increased distortion because an increased distortion leads to an additional 3T_1 character in the wave function of the emitting $(^3T_2)^3B_1$ state [Eq. (2)]. Since the oscillator strength of the 3T_1 state is ~ 20 times larger than the oscillator strength of the 3T_2 state in Cr^{4+} systems [2,4,29], increased 3T_1 mixing enhances the radiative decay rate of the $(^3T_2)^3B_1$ state.

In addition to influencing the $(^3T_2)^3B_1$ radiative decay rate, enhanced 3T_1 mixing can also influence the line shape of emission from the $(^3T_2)^3B_1$ state. The $(^3T_2)^3B_1$ line shape will be affected if the 3T_1 state interacts differently with the lattice than the $(^3T_2)^3B_1$ state. In all Cr^{4+} systems reported to date, the 3T_1 state is known to exhibit a large Franck-Condon offset relative to the 3A_2 ground state. S values between 2 and 3 are typically observed [2–4,17,18]. As a result, strong 3T_1 mixing can be expected to lead to

an increase in S in Cr^{4+} systems whose 3T_2 emission in the absence of 3T_1 mixing is sharp.

The substantial reduction in the magnitude of the blueshift of the $(^3T_2)^3B_1$ emission observed above ~ 70 kbar in $\text{Cr}^{4+}:\text{Mg}_2\text{SiO}_4$ indicates that a significant increase in the nontetrahedral distortion occurs above ~ 70 kbar. The development of the broad emission intensity between ~ 70 and ~ 120 kbar is also consistent with a significant increase in the nontetrahedral distortion because a more pronounced distortion leads to greater 3T_1 - 3T_2 electronic mixing and greater 3T_1 character in the emitting $(^3T_2)^3B_1$ state [Eq. (2)]. We attribute the large increase in S (Figs. 2a and 3) with pressure to greater 3T_1 - 3T_2 mixing. The influence of the 3T_1 state is also reflected in the change in coupling phonon. At ambient pressure, vibronic coupling in $\text{Cr}^{4+}:\text{Mg}_2\text{SiO}_4$ occurs primarily through the symmetric stretching mode $\nu_1(a_1)$ ($\sim 750 \text{ cm}^{-1}$) [2–4,6,7,17,18]. The coupling mode associated with the broad emission band ($\sim 430 \text{ cm}^{-1}$), on the contrary, corresponds to a bending mode $\nu_2(e)$ [30]. The difference in coupling mode is consistent with a strong influence of another electronic state on the emission properties of the $(^3T_2)^3B_1$ state.

The decrease in broad emission intensity observed above ~ 120 kbar is accompanied by a reversal of shift direction and coalescence of spectral intensity into a new emission feature E_1 (Fig. 2b). We attribute these spectral changes to a $(^3T_2)^3B_1$ - 1E electronic crossover and assign the E_1 line to a transition from the lowest orbital 1E component to the 3A_2 ground state. Since the energy of the 1E state depends primarily on covalency effects, a redshift of the 1E barycenter with pressure is expected on the basis of the nephelauxetic effect. This redshift, coupled with the weak blueshift of the $(^3T_2)^3B_1$ state, is responsible for the crossover. Recent results reported for isoelectronic Mn^{5+} [10,13] and angular overlap model calculations on $\text{Cr}^{4+}:\text{Y}_3\text{Al}_5\text{O}_{12}$ [8] also indicate that an increased distortion increases the splitting of the 1E state and augments the redshift of its lowest orbital component (1A_1). This effect further facilitates the $(^3T_2)^3B_1$ - 1E electronic crossover. Back-extrapolation of the 1E energy and shift at high pressure allows us to estimate an energy of $\sim 9560 \text{ cm}^{-1}$ for the lowest 1E orbital state at ambient pressure.

Our results illustrate the central role of nontetrahedral distortions on the emission properties of the 3T_2 state of Cr^{4+} . The presence of the distortion leads not only to simple splittings of the $3d^2$ electronic states but also enables 3T_1 - 3T_2 electronic mixing. Since the 3T_1 state has a much higher oscillator strength and much stronger lattice coupling than the 3T_2 state, this mixing has a profound

influence on the line shape and dynamic luminescence properties of $3d^2$ emitting systems. Our results indicate that Cr^{4+} will exhibit broad 3T_2 emission when it occupies highly distorted tetrahedral bonding sites and sharp line emission when it occupies regular or weakly distorted tetrahedral sites. Spectral transformations from sharp line 3T_2 emission to broadband 3T_2 emission (or vice versa) can be expected when variations in pressure, temperature, or composition sufficiently increase (or decrease) the extent of nontetrahedral distortions.

Our results also show that the 1E state is $\sim 400\text{ cm}^{-1}$ higher in energy than the emitting $({}^3T_2){}^3B_1$ state at ambient pressure. As a result, interactions between the 1E and 3T_2 states are expected to be weak and it seems unlikely that 1E - 3T_2 mixing is responsible for the narrow 3T_2 emission features observed at ambient pressure [2,4].

In summary, our results demonstrate the importance of the higher excited 3T_1 state of Cr^{4+} in determining the emission properties of the first excited 3T_2 state. The influence of the 3T_1 state is controlled by the extent of its electronic mixing with the 3T_2 state and this mixing is directly related to the magnitude of nontetrahedral distortions present at the Cr^{4+} site. The important influence of the 3T_1 state has been revealed by using pressure to systematically increase the nontetrahedral distortion of $\text{Cr}^{4+}:\text{Mg}_2\text{SiO}_4$. The larger distortions observed at high pressure enabled strong 3T_1 - 3T_2 electronic mixing and were responsible for a transformation from a sharp line 3T_2 spectrum at ambient pressure to a broad 3T_2 spectrum at high pressure. It is the ability to observe a range of distortions in one system at different pressures that has allowed us to elucidate the important influence of nontetrahedral distortions on the spectral properties of Cr^{4+} in different host lattices at ambient pressure.

Our results show more generally that geometric distortions represent a new degree of freedom in controlling the luminescence properties of transition metal dopants. Distortions from regular symmetry are customarily viewed in terms of their effect on crystal field splittings. Our results show that low-symmetry distortions can also enable electronic mixing processes that significantly alter the line shapes and radiative decay rates of spectral transitions. As a result, controlled structural perturbations of coordination environments of luminescent centers become a viable new direction in the design of new optical materials. Cr^{4+} represents the first system in this direction.

We gratefully acknowledge primary financial support from the National Science Foundation through Grant No. DMR-9629990. Partial financial support was also provided by WSU's Institute for Shock Physics through Grant No. DE-FG03-97SF21388 from the Department of Energy. We thank Professor U. Hömmerich for his initial

experiments, Dr. Larry Merkle for kindly providing the sample of $\text{Cr}^{4+}:\text{Mg}_2\text{SiO}_4$, and Dr. Toni Riedener for his valuable insight.

-
- [1] V. Petričević, S.K. Gayen, and R.R. Alfano, *Appl. Opt.* **27**, 4162 (1988).
 - [2] W. Jia *et al.*, *Phys. Rev. B* **43**, 5234 (1991).
 - [3] S.G. Demos and R.R. Alfano, *Phys. Rev. B* **46**, 8811 (1992).
 - [4] M.F. Hazenkamp *et al.*, *Phys. Rev. B* **53**, 2367 (1996).
 - [5] S. Kück *et al.*, *Phys. Rev. B* **51**, 17323 (1995).
 - [6] M. Atanasov, *Chem. Phys. Lett.* **234**, 313 (1995).
 - [7] K. Wissing *et al.*, *Solid State Commun.* **108**, 1001 (1998).
 - [8] M.J. Riley *et al.*, *Phys. Rev. B* **59**, 1850 (1999).
 - [9] U. Hömmerich *et al.*, *J. Lumin.* **55**, 293 (1993).
 - [10] U. Oetliker *et al.*, *J. Chem. Phys.* **100**, 8656 (1994).
 - [11] T. Brunold, A. Hauser, and H.U. Güdel, *J. Lumin.* **59**, 321 (1994).
 - [12] J.A. Capobiano *et al.*, *J. Lumin.* **54**, 1 (1992).
 - [13] M.A. Scott *et al.*, *J. Phys. Condens. Matter* **9**, 9893 (1997).
 - [14] L.D. Merkle, Y. Guyot, and B.H.T. Chai, *J. Appl. Phys.* **77**, 474 (1994).
 - [15] N. Zhavoronkov, A. Avtikh, and V. Mikhailov, *Appl. Opt.* **36**, 8601 (1997).
 - [16] S.M. Giffin and I.T. McKinnie, *Opt. Lett.* **24**, 884 (1999).
 - [17] T. Togashi *et al.*, *Appl. Phys. B* **68**, 169 (1999).
 - [18] D.M. Calistru, S.G. Demos, and R.R. Alfano, *Phys. Rev. Lett.* **78**, 374 (1997).
 - [19] A. Regev and J.H. Freed, *J. Chem. Phys.* **103**, 5315 (1995).
 - [20] W. Jia *et al.*, *J. Lumin.* **59**, 279 (1994).
 - [21] Y.R. Shen, U. Hömmerich, and K.L. Bray, *Phys. Rev. B* **56**, R473 (1997).
 - [22] The identity of the lowest energy component of the 3T_2 excited state has not been firmly established. In C_{2v} symmetry, the 3T_2 state splits into 3B_1 , 3B_2 , and 3A_2 states. 3A_2 [2] and 3B_2 [20] have been proposed as the lowest energy component. The calculations we present in this paper predict that the 3B_1 component is lowest in energy. We accordingly assume that emission occurs from the $({}^3T_2){}^3B_1$ state while recognizing that agreement over the ordering of the 3T_2 components has not been reached.
 - [23] T.S. Rose *et al.*, *J. Opt. Soc. Am. B* **11**, 428 (1994).
 - [24] C.W. Struck and W.H. Fonger, *Understanding Luminescence Spectra and Efficiency Using and Related Functions* (Springer-Verlag, Berlin, 1991).
 - [25] The notation $|(et_2){}^3T_2{}^3E{}^3B_1\rangle$ identifies electronic states according to the $T_d \rightarrow D_{2d} \rightarrow C_{2v}$ distortion scheme discussed in the text.
 - [26] S.J. Duclos, Y.K. Vohra, and A.L. Ruoff, *Phys. Rev. B* **41**, 5372 (1990).
 - [27] D. Galanciak *et al.*, *J. Lumin.* **60&61**, 223 (1994).
 - [28] U. Hömmerich and K.L. Bray, *Phys. Rev. B* **51**, 8595 (1995); **51**, 12133 (1995).
 - [29] K.V. Yumashev *et al.*, *Appl. Phys. Lett.* **70**, 2523 (1997).
 - [30] D.M. Calistru *et al.*, *Phys. Rev. B* **51**, 14980 (1995).